JPET Fast Forward. Published on August 16, 2019 as DOI: 10.1124/jpet.119.260489
This article has not been copyedited and formatted. The final version may differ from this version.

A pharmacokinetic natural product-disease-drug interaction: a double hit of silymarin and nonalcoholic steatohepatitis on hepatic transporters in a rat model

Michelle L. Montonye, Dan-Dan Tian, Tarana Arman, Katherine D. Lynch, Bruno Hagenbuch, Mary F. Paine, John D. Clarke

Department of Pharmaceutical Sciences, Washington State University, Spokane, WA, 99202 (M.L.M., T.A., D.D.T., K.D.L, K.C., M.F.P., J.D.C.); Department of Pharmacology, Toxicology and Therapeutics, The University of Kansas Medical Center, Kansas City, Kansas 66160 (B.H.)

Running title: Pharmacokinetic natural product-disease-drug interaction

Corresponding author:

John D. Clarke

Pharmaceutical and Biomedical Sciences Building

412 East Spokane Falls Blvd

Spokane, WA 99202

j.clarke@wsu.edu

Phone: 509-358-7929

Manuscript content:

Number of text pages: 36

Number of tables: 1

Number of figures: 8

Number of references: 40

Abstract: 226

Introduction: 503

Discussion: 1316

Nonstandard abbreviations: area under the plasma concentration-time curve (AUC); breast cancer resistance protein (BCRP); systemic clearance (Cl); extracellular signal-regulated kinase (Erk); methionine and choline deficient (MCD); multidrug resistance-associated protein (MRP); nonalcoholic fatty liver disease (NAFLD); nonalcoholic steatohepatitis (NASH); organic anion transporting polypeptide (OATP); apparent volume of distribution at steady state (V_{ss})

Recommended section: Metabolism, Transport, and Pharmacogenomics

JPET Fast Forward. Published on August 16, 2019 as DOI: 10.1124/jpet.119.260489
This article has not been copyedited and formatted. The final version may differ from this version.

Abstract

Patients with nonalcoholic steatohepatitis (NASH) exhibit altered hepatic protein expression of metabolizing enzymes and transporters and altered xenobiotic pharmacokinetics. The botanical natural product silymarin, which has been investigated as a treatment for NASH, contains flavonolignans that inhibit organic anion transporting polypeptide (OATP) transporter function. The purpose of this study was to assess the individual and combined effects of NASH and silymarin on the disposition of the model OATP substrate pitavastatin. Male Sprague Dawley rats were fed a control or a methionine and choline deficient diet (NASH model) for 8 weeks. Silymarin (10 mg/kg) or vehicle, followed by pitavastatin (0.5 mg/kg), were administered intravenously, and the pharmacokinetics were determined. NASH increased mean total flavonolignan area under the plasma concentration-time curve ($AUC_{0\text{-}120min}$) 1.7-fold. Silymarin increased pitavastatin $AUC_{0\text{-}120min}$ in both control and NASH animals ~2-fold. NASH increased pitavastatin plasma concentrations from 2-40 minutes, but $AUC_{0\text{-}120min}$ was unchanged. The combination of silymarin and NASH had the greatest effect on pitavastatin $AUC_{0\text{-}120min}$, which increased 2.9-fold compared to control vehicle-treated animals. NASH increased the total amount of pitavastatin excreted into the bile 2.7-fold compared to control animals, whereas silymarin decreased pitavastatin biliary clearance ~3-fold in both control and NASH animals. This double hit of NASH and silymarin on hepatic uptake transporters is another example of a multifactorial pharmacokinetic interaction that may have a greater impact on drug disposition than each hit alone.

Significance statement: Multi-factorial effects on xenobiotic pharmacokinetics are within the next frontier for precision medicine research and clinical application. The combination of silymarin and NASH is a probable clinical scenario that can affect drug uptake, liver concentrations, biliary elimination, and ultimately, efficacy and toxicity.

JPET Fast Forward. Published on August 16, 2019 as DOI: 10.1124/jpet.119.260489
This article has not been copyedited and formatted. The final version may differ from this version.

Introduction

Nonalcoholic steatohepatitis (NASH) is a severe form of nonalcoholic fatty liver disease (NAFLD) (Chalasani *et al.*, 2018). An emerging concern for NASH patients is altered expression and function of drug metabolizing enzymes and transporters, potentially leading to altered pharmacokinetics of xenobiotics. For example, previous studies suggested that decreased sinusoidal expression of hepatic organic anion transporting polypeptide (OATP) uptake transporters may be responsible for the net 1.4-fold increase in systemic concentrations of ^{99m}Tc-mebrofenin observed in NASH patients (Clarke *et al.*, 2017; Ali *et al.*, 2018). In addition, impaired canalicular localization of the efflux transporter multidrug resistance-associated protein (MRP)2 and increased sinusoidal expression of MRP3 may be responsible for higher plasma retention of morphine glucuronides in rodent models of NASH and in NASH patients (Hardwick *et al.*, 2011, 2012, 2013; Dzierlenga *et al.*, 2015; Ferslew *et al.*, 2015). These changes in xenobiotic disposition may alter therapeutic and adverse drug responses in NASH patients.

The high clinical burden of NAFLD has spurred investigation of novel therapeutic agents, including the botanical natural product silymarin. Silymarin, an extract prepared from the seeds of milk thistle (*Silybum marianum* (L.) Gaertn.), and other milk thistle preparations have been used for centuries to treat liver and gallbladder disorders (Abenavoli *et al.*, 2010). Milk thistle has remained within the top 20 best-selling herbal dietary supplements in the U.S. mainstream multi-outlet channel for the past 30 years, with 16.8 million dollars in sales in 2017 (Smith *et al.*, 2018). Evidence for the efficacy of silymarin in NAFLD patients is limited, although incorporation of silymarin into treatment

JPET Fast Forward. Published on August 16, 2019 as DOI: 10.1124/jpet.119.260489
This article has not been copyedited and formatted. The final version may differ from this version.

plans, either alone or in combination with other agents, continues to be investigated (Abenavoli and Bellentani, 2013). Multiple studies have demonstrated that silymarin is well tolerated at doses greater than one gram and, in NAFLD patients specifically, silymarin doses of 700 mg three times daily have been used safely (Hawke *et al.*, 2010; Abenavoli and Bellentani, 2013; Colica *et al.*, 2017; Fathalah *et al.*, 2017; Wah Kheong *et al.*, 2017). Thus, NAFLD patients are a target population for silymarin use and may be taking more than the 140 mg dose that is commonly recommended (Zhu *et al.*, 2013). In vitro studies indicate that silymarin, which is a complex of at least 7 flavonolignans, inhibits human OATP1B1, OATP1B3, and OATP2B1 (IC_{50}, 0.3-3.2 μM) and the canalicular efflux transporter, breast cancer resistance protein (BCRP) (K_i, 97 μM) (Deng *et al.*, 2008; Köck *et al.*, 2013).

The objective of this study was to determine the effects of NASH and silymarin, both alone and in combination, on the pharmacokinetics of the clinical OATP probe substrate pitavastatin (Prueksaritanont *et al.*, 2014). Using an established rat model of NASH (Canet *et al.*, 2014), the study was designed to mimic systemic concentrations of silymarin flavonolignans in NAFLD patients taking 700 mg of silymarin. An intravenous administration route was selected to isolate hepatic uptake and efflux processes by bypassing potential variability in oral absorption of pitavastatin and silymarin. Results suggest that the presence of NASH may increase the risk for this OATP-mediated natural product-disease-drug interaction.

Materials and Methods

Animals

Handling, care, and maintenance of the animals took place in the Program of the Laboratory Animal Resources facility of Washington State University, Spokane, which is an Association for the Assessment of Laboratory Animal Care International accredited institution. All animals were maintained in 12-hour light and dark cycles for the duration of the study. The experimental protocol was approved by the Institutional Animal Care and Use Committee at Washington State University. Eight week old male Sprague-Dawley rats (n=16) were purchased from Envigo (Huntingdon, Cambridgeshire, United Kingdom). Animals were randomly placed in cages (2 per cage) with diamond soft paper bedding and fed either a control diet (Cat. # D518754, Dyets Inc., Bethlehem, PA) or a methionine and choline deficient (MCD) diet (Cat. # D518810, Dyets Inc.). The latter diet is the best rat model for assessing alterations in drug transporters and drug disposition observed in clinical NASH (Canet *et al.*, 2014).

After eight weeks of diet, animals were anesthetized via intraperitoneal injection of ketamine (87 mg/kg, 1 mL/kg) and xylazine (13 mg/kg, 1 mL/kg). Body temperature was maintained with heated surgical tables and monitored with a rectal thermometer. The trachea was surgically exposed, and a tracheotomy was performed by inserting PE240 tubing (Braintree Scientific, Braintree, MA) into the trachea. Isoflurane (1.5%) was administered through a small animal ventilator (Kent Scientific, Torrington, CT) to maintain anesthesia and oxygen through the remainder of the study. The carotid artery and jugular vein were cannulated with PE50 tubing (Braintree Scientific), and the common bile duct was cannulated with PE10 tubing (Braintree Scientific).

Silymarin (Sigma Aldrich, St. Louis, MO; Cat. #S0292, lot #BCBT9170) was dissolved in sterile saline with 15% ethanol and 30% PEG400 by heating to 37°C and homogenized with a vortex mixer. Pitavastatin acid, hereafter referred to as pitavastatin (Abcam, Cambridge, MA; Cat. #ab141958), was dissolved in dimethyl sulfoxide (DMSO) and diluted in sterile saline (2% DMSO final). Silymarin and pitavastatin were prepared fresh daily. The total time for silymarin and pitavastatin administration into the jugular vein was two minutes. Silymarin or vehicle was administered first (10 mg/kg, 1 mL/kg), immediately followed by pitavastatin (0.5 mg/kg, 1 ml/kg).

Blood (~100 µL) was collected into heparinized tubes at 2, 5, 10, 20, 40, 80, and 120 minutes after silymarin/pitavastatin administration, and bile was collected in 15-minute increments. Plasma was isolated by centrifugation (10,000 x g for 5 min at 4°C). Interconversion between the acid and lactone forms of pitavastatin was prevented by acidifying plasma and bile samples with ammonium acetate (pH 4.2) at a volume ratio of 1 to 15 (acid to biological sample) immediately after collection (Qi *et al.*, 2013). After the final blood collection, animals were euthanized via exsanguination. Liver and muscle tissues were collected, snap frozen in liquid nitrogen, and stored at -80°C until further analyses.

Western blot analysis

Liver tissues were homogenized in NP-40 lysis buffer with protease inhibitors (cOmplete™ Protease Inhibitor Cocktail; Roche, Basel, Switzerland) (100 mg tissue/1 mL buffer) using a TissueLyzer II (Qiagen, Hilden, Germany) with 2 metal beads (2.4 mm) and the following protocol: 30 Hz for 3 minutes, transfer to ice for 5 minutes, 30 Hz for 3 minutes. Cellular debris was removed by centrifugation at 15,000 x g for 10 minutes at

JPET Fast Forward. Published on August 16, 2019 as DOI: 10.1124/jpet.119.260489
This article has not been copyedited and formatted. The final version may differ from this version.

4°C. Ten micrograms of total protein were loaded into 7.5% SDS-PAGE gels and transferred to PVDF membranes with a Bio-Rad (Hercules, CA) Trans-Blot Turbo system at 25 V/1.0 amp for 30 minutes. Membranes were blocked with 5% nonfat dry milk in Tris-buffered saline/Tween 20 and incubated with the following antibody conditions: OATP1B2 (Santa Cruz Biotechnology, Santa Cruz, CA; Cat. # 376904, 1:1,000; mouse secondary 1:10,000) and extracellular signaling-regulated kinase (Erk) 1 and 2 (Santa Cruz Biotechnology, Cat. # 271269 and # 1647; 1:20,000). Signal was developed with SuperSignal West Femto (ThermoFisher Scientific, Waltham, MA) and images captured using a Bio-Rad ChemiDoc imager. Densitometry was performed using ImageJ software (National Institutes of Health, Bethesda MD).

Liquid chromatography/mass spectrometry for pitavastatin

Quantification of pitavastatin was adapted from published methods (Qi *et al.*, 2013). Chromatographic separation and quantification was performed on a QTRAP 6500 UHPLC-MS/MS system (AB Sciex, Framingham, MA). A gradient of 0.1% formic acid in water (A) and 0.1% formic acid in acetonitrile (B) was passed through an HSS T3 column (1.8 µm, 2.1 x 50 mm) (Waters Corporation, Waltham, MA) at 50°C under the following conditions: 0-1 minute, ramp from 50% to 78% B; 1-1.5 minutes 90% B; 1.5-2 minutes, 50% B; flow rate 0.5 mL/min. The auto-sampler was maintained at 4°C, and the sample injection volume was 2 µL. The turbo electrospray source was operated in the positive ionization mode. The following parameters in multiple reaction monitoring were used for compound detection: pitavastatin, 422.1 → 290.1 m/z, declustering potential (DP) 111 volts, collision energy (CE) 37 volts; pitavastatin lactone (Cayman Chemicals, Ann Arbor, MI), 404.1 → 290.1 m/z, DP 111 volts, CE 35 volts; pitavastatin-d_5 (Toronto Research

JPET Fast Forward. Published on August 16, 2019 as DOI: 10.1124/jpet.119.260489
This article has not been copyedited and formatted. The final version may differ from this version.

Chemicals, Ontario, Canada), 426.9 → 293.8 m/z, DP 136 volts, CE 41 volts; pitavastatin lactone-d_5 (Toronto Research Chemicals), 409.1 → 295.2, DP 81 volts, CE 37 volts. Plasma and bile samples were processed by mixing 10 µL of plasma or 10 µL of pre-diluted bile (20-fold) in water with 50 µL of 0.1% formic acid in water containing 0.24 µM pitavastatin-d_5 and 1.24 µM pitavastatin lactone-d_5 deuterated internal standards, followed by addition of 40 µL of 0.1% formic acid in acetonitrile. Samples were homogenized with a vortex mixer and centrifuged at 13,000 x g for 10 minutes at 4°C. The supernatant was transferred to an auto-sampler vial for analysis. Liver samples were pulverized with a mortar and pestle under liquid nitrogen. Powdered tissue was mixed with 0.1% formic acid in water containing 1.2 µM pitavastatin-d_5 and 6.2 µM pitavastatin lactone-d_5 deuterated internal standards at a ratio of 50 mg tissue to 100 µL of 0.1% formic acid in water and homogenized with a vortex mixer. The mixture was snap frozen in liquid nitrogen, thawed, homogenized with a vortex mixer, and centrifuged at 13,000 x g for 10 minutes at 4°C. Ten microliters of the supernatant were mixed with 80 µL of 0.1% formic acid in acetonitrile, homogenized with a vortex mixer, and centrifuged at 13,000 x g for 10 minutes at 4°C. The clean supernatant (70 µL) was transferred to an auto-sampler vial for analysis. Quantification of unknowns was accomplished using a calibration curve that was linear from 0.018 to 4.75 µM and quality control samples were run periodically to ensure consistent instrument performance.

Liquid chromatography/mass spectrometry for silymarin flavonolignans

Quantification of silymarin flavonolignans was adapted from previous methods (Gufford *et al.*, 2014). All purified standards were provided by Dr. Nicholas Oberlies (University of North Carolina at Greensboro, Greensboro, NC). The same UPLC-MS/MS

system and column used for pitavastatin was used for silymarin flavonolignans. A gradient of 0.1% formic acid in water (A) and 0.1% formic acid in methanol (B) at 50°C was used under the following conditions: 0-0.1 minute, ramp from 5% to 30% B; 0.1-5.5 minutes ramp from 30% to 53% B; 5.5-6.5 minutes, 5% B; flow rate 0.5 mL/min. The auto-sampler was maintained at 4°C, and the sample injection volume was 10 µL. The turbo electrospray source was operated in the negative ionization mode. The following parameters in multiple reaction monitoring were used for compound detection: silybin A, 480.9 → 301.9 m/z, DP -30 volts, CE -26 volts; silybin B, 480.9 → 125.0 m/z, DP -5 volts, CE -34 volts; silychristin, 480.9 → 325.1 m/z, DP -5 volts, CE -30 volts; silydianin, 480.9 → 178.9 m/z, DP -50 volts, CE -32 volts; isosilybin A, 480.9 → 125.0 m/z, DP -70 volts, CE -34 volts; isosilybin B, 480.9 → 125.0 m/z, DP -10 volts, CE -34 volts; isosilychristin, 480.9 → 463.0, DP -30 volts, CE -22 volts; taxifolin, 302.8 → 284.9 m/z, DP -15 volts, CE -16 volts; all silybin β-glucuronides, 657.1 → 481.1, DP -25 volts, CE -25 volts; naringin, 578.9 → 270.9, DP -25 volts, CE -44 volts. Because chromatographic separation of the silybin A and silybin B forms of the 7-*O*-β-glucuronides could not be achieved, these compounds were quantified together and referred to as silybinin-7-*O*-β-glucuronides. Plasma samples were processed by mixing 20 µL of plasma with 50 µL of naringin (0.17 µM) as internal standard, followed by addition of 30 µL of 0.1% formic acid in methanol. Samples were homogenized with a vortex mixer and centrifuged at 13,000 x g for 10 minutes at 4°C. The clean supernatant (70 µL) was transferred to an auto-sampler vial for analysis. In addition, an aliquot of the silymarin solution administered in the animal study was analyzed using these methods to determine the flavonolignan composition of the dose. Quantification of unknowns was accomplished using a calibration curve that

JPET Fast Forward. Published on August 16, 2019 as DOI: 10.1124/jpet.119.260489
This article has not been copyedited and formatted. The final version may differ from this version.

was linear from 0.016 µM to 4.16 µM and quality control samples were run periodically to ensure consistent instrument performance.

Pharmacokinetic analysis

The pharmacokinetics of the silymarin flavonolignans and pitavastatin were determined via noncompartmental methods using Phoenix WinNonlin (version 7.0, Certara, Princeton, NJ). AUC from 0 to 120 min ($AUC_{0\text{-}120min}$) was determined using the logarithmic trapezoidal method. Terminal slope (λ_z) was calculated via linear regression of at least the last three data points. AUC from 0 to infinite time ($AUC_{0\text{-}inf}$) was calculated as the sum of $AUC_{0\text{-}120min}$ and the ratio of the concentration at 120 min to λ_z. Systemic clearance (Cl) was calculated as the ratio of dose to $AUC_{0\text{-}inf}$. Volume of distribution at steady state (V_{ss}) was calculated as the product of Cl and mean residence time (MRT), where MRT is the ratio of area under the moment curve from zero to infinite time to $AUC_{0\text{-}inf}$. Terminal half-life ($t_{1/2}$) was calculated as the ratio of 0.693 to λ_z. One of the silymarin treated NASH animals received the incorrect dose of pitavastatin and was excluded from pitavastatin analyses because the actual dose could not be determined with confidence.

IC_{50} determination

All cells were maintained at 37°C in a humidified 5% CO_2 atmosphere. Human embryonic kidney (HEK)293T/17 cells were seeded at 1.5 x 10^5 cells per well onto poly-d-lysine coated 12-well plates and were transiently transfected with 0.75 µg of rat OATP1B2-expressing plasmid (pcDNA5/FRT vector) for 4 hours using jetPRIME (Polyplus Transfection, Illkirch, France). After incubation, the medium was changed to fresh medium with no transfection reagent. Cells were grown for an additional 24 hours

JPET Fast Forward. Published on August 16, 2019 as DOI: 10.1124/jpet.119.260489
This article has not been copyedited and formatted. The final version may differ from this version.

before performing the transport assays. Chinese hamster ovary (CHO) cells stably expressing human OATP1B1 or OATP1B3 were provided by Dr. Bruno Stieger (University of Zurich, Zurich, Switzerland). CHO cells were grown in Dulbecco's Modified Eagle Medium (low glucose) containing 25 mM HEPES, supplemented with 10% fetal bovine serum, and 50 µg/mL L-proline. Cells were seeded onto 12-well plates at a density of 1 x 10^5 cells per well. Transporter expression was induced in CHO cells by adding 5 mM sodium butyrate to the culture media for 24 hours before performing transport experiments. Cells were washed with pre-warmed uptake buffer (135 mM sodium chloride, 1.3 mM HEPES, 2.8 mM D-glucose, 0.5 mM potassium chloride, 0.25 mM calcium dichloride, 0.12 mM magnesium dichloride, 80 µM magnesium sulfate, pH 7.4) three times and allowed to equilibrate in the final wash for 5 minutes. Uptake was initiated by addition of pre-warmed transport buffer containing 1 µM pitavastatin, and transport was terminated at 3 minutes by adding ice cold uptake buffer. Cells were washed quickly three times with ice cold uptake buffer before being lysed with 110 µL of HPLC water. Plates were subjected to a freeze-thaw cycle at -80°C before the wells were scraped and the sample transferred to a microcentrifuge tube. Eighty µL of the supernatant were mixed with 320 µL of acetonitrile containing 0.04 µM pitavastatin-d_5 and 0.2 µM pitavastatin lactone-d_5. Samples were homogenized with a vortex mixer and centrifuged at 13,000 x g for 5 minutes at room temperature. The supernatant (380 µL) was dried under vacuum at 37°C, then reconstituted in 50 µL of 20% acetonitrile with 0.1% formic acid and analyzed for pitavastatin as described above. Transport in wild-type CHO and empty vector transfected HEK293T/17 cells was subtracted from transport in OATP-expressing cells and are presented as percent of control. Best-fit IC_{50} values were determined by

JPET Fast Forward. Published on August 16, 2019 as DOI: 10.1124/jpet.119.260489
This article has not been copyedited and formatted. The final version may differ from this version.

nonlinear least-squares regression using Phoenix WinNonlin (v. 8.1; Certara, St. Louis, MO) as described previously (Gufford *et al.*, 2014).

Statistical analysis

All data represent mean ± S.E.M. Two-way ANOVA p-values are shown in tables accompanying the respective graph. Tukey's post hoc test was used to compare groups: a = p-value ≤ 0.05 versus respective vehicle group within each diet group; b = p-value ≤ 0.05 versus vehicle control; c = p-value ≤ 0.05 versus silymarin control. Comparisons of silymarin flavonolignans between control and NASH groups were made using the unpaired Student's t-test.

JPET Fast Forward. Published on August 16, 2019 as DOI: 10.1124/jpet.119.260489
This article has not been copyedited and formatted. The final version may differ from this version.

Results

Pharmacokinetics of silymarin flavonolignans

The percent extrapolation from $AUC_{0\text{-}120min}$ to $AUC_{120min\text{-}inf}$ for the silymarin flavonolignans ranged from 0.23% to 18%. Average $AUC_{0\text{-}inf}$ of silybin A, silybin B, isosilybin A, and isosilybin B was 1.5 to 2.0-fold higher in the NASH group compared to the control group (Fig. 1, Table 1). Cl of each flavonolignan decreased by 40-69% in the NASH group compared to the control group (Table 1). The terminal $t_{1/2}$ of silybin B and isosilybin A increased 1.7- and 1.8-fold, respectively, in the NASH group compared to the control group. V_{ss} of each flavonolignan decreased by 40-69% in the NASH group compared to the control group.

Average $AUC_{0\text{-}120min}$ of silybin A-4''-*O*-β-glucuronide, silybin B-4''-*O*-β-glucuronide, and silybinin-7-*O*-β-glucuronide was approximately 2-fold higher in the NASH group compared to the control group (Fig. 2). Average total flavonolignan $AUC_{0\text{-}120min}$ (flavonolignans plus glucuronides) increased 1.7-fold in the NASH group compared to the control group (594 ± 71 versus 353 ± 32 nmol x min/mL, mean ± S.E.M.) ($p<0.001$).

Pharmacokinetics of pitavastatin

Pitavastatin lactone was below the detection limit in all samples. The NASH vehicle group showed higher pitavastatin concentrations from 2 to 40 minutes but did not significantly change $AUC_{0\text{-}120min}$ compared to the control vehicle group (Fig. 3A and B). Average pitavastatin $AUC_{0\text{-}120min}$ increased 1.8-fold in the control silymarin group and 2.9-fold in the NASH silymarin group compared to the control vehicle group (Fig. 3B). The amount of pitavastatin in bile was increased by NASH and decreased by silymarin at the

early time points (Fig. 4A). Bile flow was increased by NASH and decreased by silymarin at the early time points (Fig. 4B). The total amount of pitavastatin excreted into bile was increased due to NASH and decreased by silymarin in both control and NASH groups (Fig. 4C). Pitavastatin biliary clearance was decreased ~70% by silymarin in both control and NASH groups (Fig. 4D). The amount of pitavastatin in bile was associated with bile flow (Fig. 4E and F). At the terminal time point, the total amount of pitavastatin in the liver and the pitavastatin liver-to-plasma ratio were lower in the NASH groups (Fig. 5A and B). Total pitavastatin in the gastrocnemius (leg muscle) and pitavastatin muscle-to-plasma ratio were not different between the groups (Fig. 5C and D).

OATP1B2 protein expression in NASH and inhibitory effects of silymarin on OATPs

OATP1B2 protein expression decreased in the NASH groups but was not altered 120 minutes after a single dose of silymarin (Fig. 6). Silymarin inhibited rat OATP1B2- and human OATP1B1- and OATP1B3-mediated uptake of pitavastatin, with IC_{50} values of 13.8, 6.5, and 12.7 μM, respectively (Fig. 7).

JPET Fast Forward. Published on August 16, 2019 as DOI: 10.1124/jpet.119.260489
This article has not been copyedited and formatted. The final version may differ from this version.

Discussion

A previous clinical study reported no pharmacokinetic interaction between silymarin and an OATP substrate (rosuvastatin) in healthy subjects (Deng *et al.*, 2008). We hypothesized that the presence of NASH may increase the risk for an OATP-mediated silymarin-drug interaction compared to a healthy condition due to decreased hepatic OATP protein expression and increased systemic silymarin flavonolignan concentrations (Schrieber *et al.*, 2008; Clarke *et al.*, 2017). The present study was designed to address this hypothesis by mimicking key aspects of a clinical NAFLD scenario in an established rodent model of human NASH (Clarke *et al.*, 2014).

Pitavastatin has been proposed as an effective probe drug for OATP1B function because it is minimally metabolized and is primarily dependent on OATPs for hepatic sinusoidal uptake (Hirano *et al.*, 2004, 2005; Prueksaritanont *et al.*, 2014, 2017). Although we confirmed that silymarin inhibits rat OATP1B2, a limitation of using a rodent model to test our hypothesis is that other rodent orthologs beyond OATP1B2 (e.g., OATP1A isoforms) may be contributing to the disposition of pitavastatin (Chang *et al.*, 2019). Silymarin increased pitavastatin exposure in both the control and NASH groups, suggesting that silymarin doses at or above 700 mg may precipitate OATP-mediated drug interactions. These data are noteworthy because higher doses of silymarin, as well as milk thistle formulations designed to improve flavonolignan relative oral bioavailability, are increasingly available on the market. In addition, the combination of NASH and silymarin had the greatest effect on pitavastatin exposure, suggesting that the combined effects of NASH-mediated decrease in the protein expression of, and silymarin-mediated inhibition of, hepatic OATPs may place NASH patients at the highest risk for this OATP-mediated

JPET Fast Forward. Published on August 16, 2019 as DOI: 10.1124/jpet.119.260489
This article has not been copyedited and formatted. The final version may differ from this version.

silymarin-drug interaction. These data are consistent with a previous study indicating that a double hit on hepatic OATP-mediated uptake has a greater effect on drug exposure than each hit alone and provide additional impetus for careful evaluation of multifactorial effects on pharmacokinetics (Clarke *et al.*, 2014).

In addition to sinusoidal uptake and efflux, the current data suggest that pitavastatin biliary excretion is affected predominately by bile flow. In the NASH groups, increased bile flow likely contributed to increased pitavastatin biliary excretion. NASH alone did not increase pitavastatin biliary clearance, potentially due to variability in these data caused by capturing less than five half-lives. In the silymarin treated groups, decreased bile flow likely contributed to decreased pitavastatin biliary excretion. These opposing effects of NASH and silymarin on bile flow contrast with their combined effects on pitavastatin systemic exposure. Interestingly, the effect of bile flow on pitavastatin in bile is not a linear relationship, such that at lower pitavastatin concentrations, the relationship has a steeper slope compared to the relationship at higher concentrations. The silymarin-mediated leftward shift in the NASH pitavastatin data (Fig. 4E versus 4F) suggest that the previously reported increase in BCRP protein expression in NASH potentially plays a role in producing high pitavastatin biliary concentrations (Hardwick *et al.*, 2011; Toth *et al.*, 2018). The silymarin-mediated decrease in bile flow observed in the present study is inconsistent with a previous report showing that intraperitoneal administration of silymarin increased bile flow (Crocenzi *et al.*, 2000). The reason for this discrepancy is unclear but may be related to the strain of rats used (Wistar versus Sprague Dawley) or route of silymarin administration (intraperitoneal versus intravenous). Silymarin-mediated inhibition of BCRP is not expected to contribute to altered biliary

JPET Fast Forward. Published on August 16, 2019 as DOI: 10.1124/jpet.119.260489
This article has not been copyedited and formatted. The final version may differ from this version.

disposition of pitavastatin because of the high K_i reported against BCRP (97 μM) (Deng *et al.*, 2008). Collectively, these data indicate that opposing effects of NASH and silymarin on bile flow influence pitavastatin biliary disposition in a rodent model.

The previous clinical study that found no pharmacokinetic interaction between silymarin (140 mg three times daily) and an OATP/BCRP substrate, rosuvastatin (10 mg single dose), has a number of limitations, some of which arose after the study was completed over a decade ago (Deng *et al.*, 2008). In addition to the limitations discussed by the authors of that study, many studies performed after 2008 have used silymarin doses greater than 140 mg three times daily (e.g., 700 mg three times daily) and/or formulations that increase flavonolignan plasma concentrations and relative oral bioavailability (Kumar *et al.*, 2014; Poruba *et al.*, 2015; Liang *et al.*, 2018). These doses and formulations that can produce higher plasma concentrations coupled with the higher plasma concentrations observed in NAFLD patients, suggest that silymarin-mediated OATP substrate interactions may occur in this multifactorial scenario. Although we were able to match maximum silybin A plasma concentrations reported for NAFLD and hepatitis C virus-infected patients taking 560-700 mg of silymarin (present study: 1.7 to 2.7 μM; clinical studies: 0.9 to 4.2 μM), an important limitation to our study is that intravenous administration of silymarin produces higher plasma concentrations of the other silymarin flavonolignans than are typically observed after oral administration (Hawke *et al.*, 2010; Schrieber *et al.*, 2011; Fried *et al.*, 2012; Köck *et al.*, 2013). Without IC_{50} values for each of the flavonolignans it is difficult to determine how each flavonolignan may be contributing to the inhibition of OATPs and increased pitavastatin systemic exposure. It remains to be determined whether these current preclinical data

and the limitations of the previous clinical pharmacokinetic interaction study necessitate a reevaluation of the risk for this natural product-drug interaction.

One of the challenges facing pharmacokinetic natural product-drug interaction research is the large variability in the composition of commercially available products. The Center of Excellence for Natural Product-Drug Interaction Research (NaPDI Center) was created to address this challenge and others by developing Recommended Approaches for studying pharmacokinetic natural product-drug interactions (Paine *et al.*, 2018). In the present study, the composition of the silymarin product was characterized and compared to previously published data on the composition of other silymarin products. The product used in this study contained less than 50% silybin A and silybin B (Fig. 8), which contrasts with a silymarin capsule and another lot of silymarin from the same source, both of which contained more than 55% silybin A and silybin B (Wen *et al.*, 2008). In addition, the silymarin product used in the current study contained more than 30% silychristin, whereas all other products contained ~20% silychristin (Wen *et al.*, 2008; Hawke *et al.*, 2010). The IC_{50} values for silymarin-mediated inhibition of pitavastatin uptake by human OATP1B1 (6.5 µM) and OATP1B3 (12.7 µM) were higher than those previously reported using estrone-3-sulfate as the probe substrate (1.3 µM and 2.2 µM, respectively) (Köck *et al.*, 2013). Another group, who used a mix of disuccinated silybin A and silybin B, reported an IC_{50} of 3.3 µM for OATP1B1 and a K_i of 5 µM for OATP1B3 using estradiol 17β-glucuronide as the probe substrate (Wlcek *et al.*, 2013). These differences may reflect different compositions of the silymarin products and/or the substrate used. In addition, the higher percentage of silychristin in the the current study may have contributed to the higher IC_{50} values, as previous data suggest that silychristin may be a less potent OATP

inhibitor (Köck *et al.*, 2013). Unfortunately, a direct comparison between the previously published and current IC_{50} values cannot be made because the composition of the product used in the previous study was not reported and the probe substrates are different (Köck *et al.*, 2013). These data highlight the importance of characterizing the constituent composition of a given natural product and its interaction with the probe drug of interest in pharmacokinetic natural product-drug interaction studies.

In conclusion, these data provide further evidence that double hit pharmacokinetic interactions can have a greater effect on drug exposure than each hit alone. This may be important for patients with chronic diseases such as NASH because these patients are often subject to polypharmacy to manage and/or treat comorbidities. In addition, patients afflicted with multiple chronic diseases are more likely to take botanical dietary supplements, potentially placing these patients at the greatest risk for adverse drug effects (Dickinson and MacKay, 2014; Patel *et al.*, 2017; Chalasani *et al.*, 2018).

Acknowledgments

We gratefully acknowledge Dr. Bruno Stieger from the University of Zurich for providing the OATP1B1 and OATP1B3 expressing CHO cells used in these experiments. We are grateful to Dr. Nicholas Oberlies from the University of North Carolina at Greensboro, who provided the silymarin flavonolignan and glucuronide standards.

Authorship Contributions

Participated in research design: Montonye, Hagenbuch, Paine, Clarke

Conducted experiments: Montonye, Arman, Lynch, Clarke

Contributed new reagents or analytic tools: Not applicable

Performed data analysis: Montonye, Arman, Tian, Lynch, Hagenbuch, Clarke

Wrote or contributed to the writing of the manuscript: Montonye, Arman, Tian, Lynch, Hagenbuch, Paine, Clarke

References

Abenavoli L, and Bellentani S (2013) Milk thistle to treat non-alcoholic fatty liver disease: dream or reality? Expert Rev Gastroenterol Hepatol 7:677–9.

Abenavoli L, Capasso R, Milic N, and Capasso F (2010) Milk thistle in liver diseases: past, present, future. Phytother Res 24:1423–32.

Ali I, Slizgi JR, Kaullen JD, Ivanovic M, Niemi M, Stewart PW, Barritt AS, and Brouwer KLR (2018) Transporter-Mediated Alterations in Patients With NASH Increase Systemic and Hepatic Exposure to an OATP and MRP2 Substrate. Clin Pharmacol Ther 104:749–756.

Canet MJ, Hardwick RN, Lake AD, Dzierlenga AL, Clarke JD, and Cherrington NJ (2014) Modeling human nonalcoholic steatohepatitis-associated changes in drug transporter expression using experimental rodent models. Drug Metab Dispos 42:586–95.

Chalasani N, Younossi Z, Lavine JE, Charlton M, Cusi K, Rinella M, Harrison SA, Brunt EM, and Sanyal AJ (2018) The diagnosis and management of nonalcoholic fatty liver disease: Practice guidance from the American Association for the Study of Liver Diseases. Hepatology 67:328–357.

Chang JH, Zhang X, Messick K, Chen Y-C, Chen E, Cheong J, and Ly J (2019) Unremarkable impact of Oatp inhibition on the liver concentration of fluvastatin, lovastatin and pitavastatin in wild-type and Oatp1a/1b knockout mouse. Xenobiotica 49:602–610.

Clarke JD, Hardwick RN, Lake AD, Canet MJ, and Cherrington NJ (2014) Experimental nonalcoholic steatohepatitis increases exposure to simvastatin hydroxy acid by

decreasing hepatic organic anion transporting polypeptide expression. J Pharmacol Exp Ther 348:452–8.

Clarke JD, Novak P, Lake AD, Hardwick RN, and Cherrington NJ (2017) Impaired N-linked glycosylation of uptake and efflux transporters in human non-alcoholic fatty liver disease. Liver Int 37:1074–1081.

Colica C, Boccuto L, and Abenavoli L (2017) Silymarin: An option to treat non-alcoholic fatty liver disease. World J Gastroenterol 23:8437–8438.

Crocenzi FA, Pellegrino JM, Sánchez Pozzi EJ, Mottino AD, Rodríguez Garay EA, and Roma MG (2000) Effect of silymarin on biliary bile salt secretion in the rat. Biochem Pharmacol 59:1015–1022.

Deng JW, Shon J-H, Shin H-J, Park S-J, Yeo C-W, Zhou H-H, Song I-S, and Shin J-G (2008) Effect of silymarin supplement on the pharmacokinetics of rosuvastatin. Pharm Res 25:1807–14.

Dickinson A, and MacKay D (2014) Health habits and other characteristics of dietary supplement users: a review. Nutr J 13:14.

Dzierlenga AL, Clarke JD, Hargraves TL, Ainslie GR, Vanderah TW, Paine MF, and Cherrington NJ (2015) Mechanistic basis of altered morphine disposition in nonalcoholic steatohepatitis. J Pharmacol Exp Ther 352:462–70.

Fathalah WF, Abdel Aziz MA, Abou El Soud NH, and El Raziky MES (2017) High Dose of Silymarin in Patients with Decompensated Liver Disease: A Randomized Controlled Trial. J Interferon Cytokine Res 37:480–487.

Ferslew BC, Johnston CK, Tsakalozou E, Bridges AS, Paine MF, Jia W, Stewart PW, Barritt AS, and Brouwer KLR (2015) Altered morphine glucuronide and bile acid

disposition in patients with nonalcoholic steatohepatitis. Clin Pharmacol Ther 97:419–27.

Fried MW, Navarro VJ, Afdhal N, Belle SH, Wahed AS, Hawke RL, Doo E, Meyers CM, Reddy KR, and Silymarin in NASH and C Hepatitis (SyNCH) Study Group (2012) Effect of silymarin (milk thistle) on liver disease in patients with chronic hepatitis C unsuccessfully treated with interferon therapy: a randomized controlled trial. JAMA 308:274–82.

Gufford BT, Chen G, Lazarus P, Graf TN, Oberlies NH, and Paine MF (2014) Identification of diet-derived constituents as potent inhibitors of intestinal glucuronidation. Drug Metab Dispos 42:1675–1683.

Hardwick RN, Ferreira DW, More VR, Lake AD, Lu Z, Manautou JE, Slitt AL, and Cherrington NJ (2013) Altered UDP-glucuronosyltransferase and sulfotransferase expression and function during progressive stages of human nonalcoholic fatty liver disease. Drug Metab Dispos 41:554–61.

Hardwick RN, Fisher CD, Canet MJ, Scheffer GL, and Cherrington NJ (2011) Variations in ATP-binding cassette transporter regulation during the progression of human nonalcoholic fatty liver disease. Drug Metab Dispos 39:2395–402.

Hardwick RN, Fisher CD, Street SM, Canet MJ, and Cherrington NJ (2012) Molecular mechanism of altered ezetimibe disposition in nonalcoholic steatohepatitis. Drug Metab Dispos 40:450–60.

Hawke RL, Schrieber SJ, Soule TA, Wen Z, Smith PC, Reddy KR, Wahed AS, Belle SH, Afdhal NH, Navarro VJ, Berman J, Liu Q-Y, Doo E, and Fried MW (2010) Silymarin ascending multiple oral dosing phase I study in noncirrhotic patients with

chronic hepatitis C. J Clin Pharmacol 50:434–49.

Hirano M, Maeda K, Matsushima S, Nozaki Y, Kusuhara H, and Sugiyama Y (2005) Involvement of BCRP (ABCG2) in the biliary excretion of pitavastatin. Mol Pharmacol 68:800–7.

Hirano M, Maeda K, Shitara Y, and Sugiyama Y (2004) Contribution of OATP2 (OATP1B1) and OATP8 (OATP1B3) to the hepatic uptake of pitavastatin in humans. J Pharmacol Exp Ther 311:139–46.

Köck K, Xie Y, Hawke RL, Oberlies NH, and Brouwer KLR (2013) Interaction of silymarin flavonolignans with organic anion-transporting polypeptides. Drug Metab Dispos 41:958–65.

Kumar N, Rai A, Reddy ND, Raj PV, Jain P, Deshpande P, Mathew G, Kutty NG, Udupa N, and Rao CM (2014) Silymarin liposomes improves oral bioavailability of silybin besides targeting hepatocytes, and immune cells. Pharmacol Reports 66:788–798.

Liang J, Liu Y, Liu J, Li Z, Fan Q, Jiang Z, Yan F, Wang Z, Huang P, and Feng N (2018) Chitosan-functionalized lipid-polymer hybrid nanoparticles for oral delivery of silymarin and enhanced lipid-lowering effect in NAFLD. J Nanobiotechnology 16:64.

Paine MF, Shen DD, and McCune JS (2018) Recommended Approaches for Pharmacokinetic Natural Product-Drug Interaction Research: a NaPDI Center Commentary. Drug Metab Dispos 46:1041–1045.

Patel PJ, Hayward KL, Rudra R, Horsfall LU, Hossain F, Williams S, Johnson T, Brown NN, Saad N, Clouston AD, Stuart KA, Valery PC, Irvine KM, Russell AW, and Powell EE (2017) Multimorbidity and polypharmacy in diabetic patients with NAFLD. Medicine (Baltimore) 96:e6761.

Poruba M, Kazdová L, Oliyarnyk O, Malinská H, Matusková Z, Tozzi di Angelo I, Skop V, and Vecera R (2015) Improvement bioavailability of silymarin ameliorates severe dyslipidemia associated with metabolic syndrome. Xenobiotica 45:751–6.

Prueksaritanont T, Chu X, Evers R, Klopfer SO, Caro L, Kothare PA, Dempsey C, Rasmussen S, Houle R, Chan G, Cai X, Valesky R, Fraser IP, and Stoch SA (2014) Pitavastatin is a more sensitive and selective organic anion-transporting polypeptide 1B clinical probe than rosuvastatin. Br J Clin Pharmacol 78:587–598.

Prueksaritanont T, Tatosian D, Chu X, Railkar R, Evers R, Chavez-Eng C, Lutz R, Zeng W, Yabut J, Chan G, Cai X, Latham A, Hehman J, Stypinski D, Brejda J, Zhou C, Thornton B, Bateman K, Fraser I, and Stoch S (2017) Validation of a microdose probe drug cocktail for clinical drug interaction assessments for drug transporters and CYP3A. Clin Pharmacol Ther 101:519–530.

Qi X, Ding L, Wen A, Zhou N, Du X, and Shakya S (2013) Simple LC-MS/MS methods for simultaneous determination of pitavastatin and its lactone metabolite in human plasma and urine involving a procedure for inhibiting the conversion of pitavastatin lactone to pitavastatin in plasma and its application to a phar. J Pharm Biomed Anal 72:8–15.

Schrieber SJ, Hawke RL, Wen Z, Smith PC, Reddy KR, Wahed AS, Belle SH, Afdhal NH, Navarro VJ, Meyers CM, Doo E, and Fried MW (2011) Differences in the disposition of silymarin between patients with nonalcoholic fatty liver disease and chronic hepatitis C. Drug Metab Dispos 39:2182–90.

Schrieber SJ, Wen Z, Vourvahis M, Smith PC, Fried MW, Kashuba ADM, and Hawke RL (2008) The pharmacokinetics of silymarin is altered in patients with hepatitis C

virus and nonalcoholic Fatty liver disease and correlates with plasma caspase-3/7 activity. Drug Metab Dispos 36:1909–16.

Smith T, Kawa K, Eckl V, Morton C, and Stredney R (2018) Herbal supplement sales in US increase 8.5% in 2017, topping $8 billion. HerbalGram 62–71.

Toth EL, Li H, Dzierlenga AL, Clarke JD, Vildhede A, Goedken M, and Cherrington NJ (2018) Gene-by-Environment Interaction of Bcrp $^{-/-}$ and Methionine- and Choline-Deficient Diet–Induced Nonalcoholic Steatohepatitis Alters SN-38 Disposition. Drug Metab Dispos 46:1478–1486.

Wah Kheong C, Nik Mustapha NR, and Mahadeva S (2017) A Randomized Trial of Silymarin for the Treatment of Nonalcoholic Steatohepatitis. Clin Gastroenterol Hepatol 15:1940-1949.e8.

Wen Z, Dumas TE, Schrieber SJ, Hawke RL, Fried MW, and Smith PC (2008) Pharmacokinetics and metabolic profile of free, conjugated, and total silymarin flavonolignans in human plasma after oral administration of milk thistle extract. Drug Metab Dispos 36:65–72.

Wlcek K, Koller F, Ferenci P, and Stieger B (2013) Hepatocellular organic anion-transporting polypeptides (OATPs) and multidrug resistance-associated protein 2 (MRP2) are inhibited by silibinin. Drug Metab Dispos 41:1522–8.

Zhu H-J, Brinda BJ, Chavin KD, Bernstein HJ, Patrick KS, and Markowitz JS (2013) An assessment of pharmacokinetics and antioxidant activity of free silymarin flavonolignans in healthy volunteers: a dose escalation study. Drug Metab Dispos 41:1679–85.

Footnotes

This work was supported in part by the National Institutes of Health National Institute of Environmental Health Sciences [Grant R00ES024455]; the National Institutes of Health National Center for Complementary and Integrative Health [Grant U54AT008909]; the National Institute of General Medical Sciences [Grant R01GM077336]; and the Washington State University College of Pharmacy and Pharmaceutical Sciences.

JPET Fast Forward. Published on August 16, 2019 as DOI: 10.1124/jpet.119.260489
This article has not been copyedited and formatted. The final version may differ from this version.

Figure legends

Figure 1: Average plasma concentration-time profiles for silymarin flavonolignans following intravenous administration of silymarin to rats. Plasma concentration-time profile for silybin A (A), silybin B (B), silychristin (C), silydianin (D), isosilybin A (E), and isosilybin B (F). Open and closed circles denote control and NASH rats, respectively. Circles and error bars represent mean and S.E.M., respectively, of 4 rats per group.

Figure 2: Average plasma concentration-time profiles for silymarin glucuronides following intravenous administration of silymarin to rats. Plasma concentration-time profile for silybin A-4''-*O*-β-glucuronide (A), silybin B-4''-*O*-β-glucuronide (B), and silybinin-7-*O*-β-glucuronide (C). $AUC_{0\text{-}120min}$ for each glucuronide (D). Open and closed circles (A-C) denote control and NASH rats, respectively. Circles and error bars represent mean and S.E.M., respectively, of 4 rats per group. *p-value ≤ 0.05 versus control (unpaired t-test).

Figure 3: Pharmacokinetics of pitavastatin in control and NASH rats with or without silymarin. Average plasma concentration-time profile for pitavastatin (A) and pitavastatin $AUC_{0\text{-}120min}$ for each group (B). Circles and error bars represent mean and S.E.M., respectively, of 3 rats for the NASH silymarin group and of 4 rats for all other groups. Two-way ANOVA p-values are shown in the table. Tukey's post-hoc test: a = p-value ≤ 0.05 versus respective vehicle group within each diet group; b = p-value ≤ 0.05 versus vehicle control.

Figure 4: Biliary excretion of pitavastatin in control and NASH rats with or without silymarin. Amount of pitavastatin recovered in bile for each collection interval (A). Bile

flow for each collection interval (B). Total pitavastatin recovered in bile (C) and pitavastatin biliary clearance (D). Data in A-D represent mean and S.E.M. of 3 rats for the NASH silymarin group and of 4 rats for all other groups. Relationship between bile flow and amount of pitavastatin for the vehicle-treated (E) and silymarin-treated (F) groups. Open circles and closed circles denote individual control and NASH rats, respectively. Two-way ANOVA p-values are shown in the tables below the respective datasets. Tukey's post-hoc test: a = p-value ≤ 0.05 versus respective vehicle group within each diet group; b = p-value ≤ 0.05 versus vehicle control; c = p-value ≤ 0.05 versus silymarin control.

Figure 5: Tissue concentrations and tissue-to-plasma ratios of pitavastatin in control and NASH rats with or without silymarin. Liver pitavastatin content (A), pitavastatin liver-to-plasma ratio (B), gastrocnemius (leg muscle) pitavastatin concentrations (C), and pitavastatin muscle-to-plasma ratio at 2 hours post-dose. Bars and error bars represent mean and S.E.M., respectively, of 3 rats for the NASH silymarin group and of 4 rats for all other groups. Two-way ANOVA p-values are shown in the table. Tukey's post-hoc test: b = p-value ≤ 0.05 versus vehicle control; c = p-value ≤ 0.05 versus silymarin control.

Figure 6: OATP1B2 expression in control and NASH rats. Representative western blot for OATP1B2 and the loading control, Erk 1/2. Bars and error bars represent mean and S.E.M., respectively, of 4 rats per group. Two-way ANOVA p-values are shown in the table. Tukey's post-hoc test: b = p-value ≤ 0.05 versus vehicle control; c = p-value ≤ 0.05 versus silymarin control.

Figure 7: Silymarin inhibition of OATP1B2-, OATP1B1-, and OATP1B3-mediated uptake of pitavastatin. IC_{50} curves for OATP1B2 (A), OATP1B1 (B), and OATP1B3 (C) were obtained by measuring uptake of 1 µM pitavastatin for 3 minutes in the absence or presence of increasing silymarin concentrations. Symbols and error bars represent mean and S.E.M., respectively, of 6 replicates. Curves denote model-generated best fits to the data. IC_{50} values represent model-generated best-fit estimates ± S.E.'s of the estimates.

Figure 8: Flavonolignan constituents in the silymarin used in this study and others. Silybin A, silybin B, isosilybin A, isosilybin B, silydianin, and silychristin expressed as percent of total flavonolignan composition. Composition of silymarin powder purchased from Sigma-Aldrich, and used in the current study, was compared to that in capsules used in two separate pharmacokinetic studies and from another lot of silymarin powder purchased from Sigma-Aldrich measured by Wen *et. al.* (Wen *et al.*, 2008; Hawke *et al.*, 2010).

JPET Fast Forward. Published on August 16, 2019 as DOI: 10.1124/jpet.119.260489
This article has not been copyedited and formatted. The final version may differ from this version.

Table 1: Silymarin flavonolignan pharmacokinetics.

	$AUC_{0\text{-}inf}$ (nmol x min/mL)	$t_{1/2}$ (min)	Cl (mL/min)	V_{ss} (L)
Silybin A				
Control	18.1 ± 1.9	14.9 ± 2.4	41.8 ± 5.3	0.51 ± 0.04
NASH	27.7 ± 2.8*	29.1 ± 5.8	17.4 ± 2.1*	0.27 ± 0.03*
Silybin B				
Control	33.6 ± 2.3	20.8 ± 2.2	39.4 ± 3.2	0.61 ± 0.06
NASH	50.2 ± 5.7*	34.6 ± 4.4*	17.2 ± 1.9*	0.28 ± 0.04*
Silychristin				
Control	105.6 ± 3.7	48.1 ± 11.8	13.2 ± 0.7	0.32 ± 0.01
NASH	112.4 ± 4.2	61.2 ± 6.6	7.9 ± 0.4*	0.19 ± 0.01*
Silydianin				
Control	11.2 ± 0.6	40.2 ± 4.2	30.5 ± 1.6	0.82 ± 0.05
NASH	14.8 ± 1.8	54.2 ± 8.5	15.2 ± 1.9*	0.41 ± 0.06*
Isosilybin A				
Control	9.6 ± 0.8	17.4 ± 2.9	46.5 ± 4.5	0.69 ± 0.04
NASH	19.4 ± 1.9*	30.8 ± 4.4*	14.6 ± 1.3*	0.28 ± 0.04*
Isosilybin B				
Control	9.9 ± 0.9	21.5 ± 2.0	21.6 ± 2.3	0.38 ± 0.03
NASH	20.1 ± 1.8*	38.9 ± 8.6	6.8 ± 0.5*	0.13 ± 0.02*

The percent extrapolation from $AUC_{0\text{-}120min}$ to $AUC_{120min\text{-}inf}$ for the silymarin flavonolignans ranged from 0.23% to 18%.

JPET Fast Forward. Published on August 16, 2019 as DOI: 10.1124/jpet.119.260489
This article has not been copyedited and formatted. The final version may differ from this version.

Abbreviations: $AUC_{0\text{-}inf}$, area under the plasma concentration-time curve from time zero to infinite time; $t_{1/2}$, terminal half-life; Cl, systemic clearance; V_{ss}, volume of distribution at steady state. Data represent mean and S.E.M. of 4 rats. *p-value ≤ 0.05 versus control (unpaired t-test)

JPET Fast Forward. Published on August 16, 2019 as DOI: 10.1124/jpet.119.260489
This article has not been copyedited and formatted. The final version may differ from this version.

Figure 1

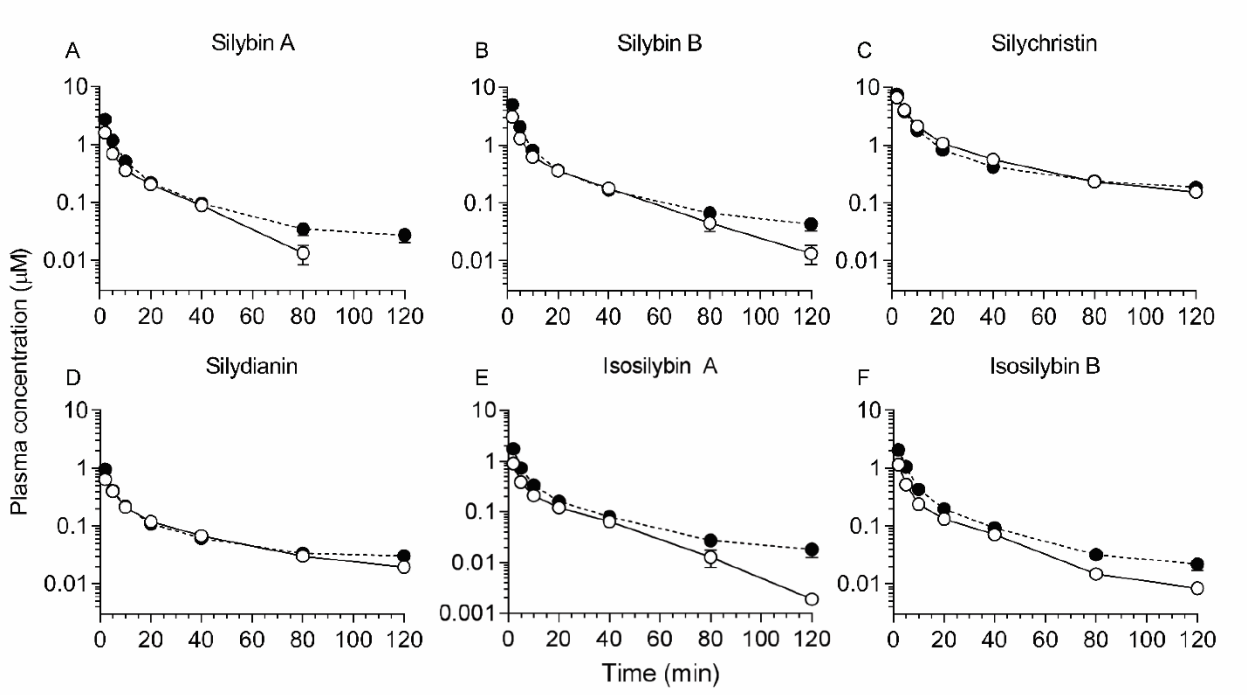

JPET Fast Forward. Published on August 16, 2019 as DOI: 10.1124/jpet.119.260489
This article has not been copyedited and formatted. The final version may differ from this version.

Figure 2

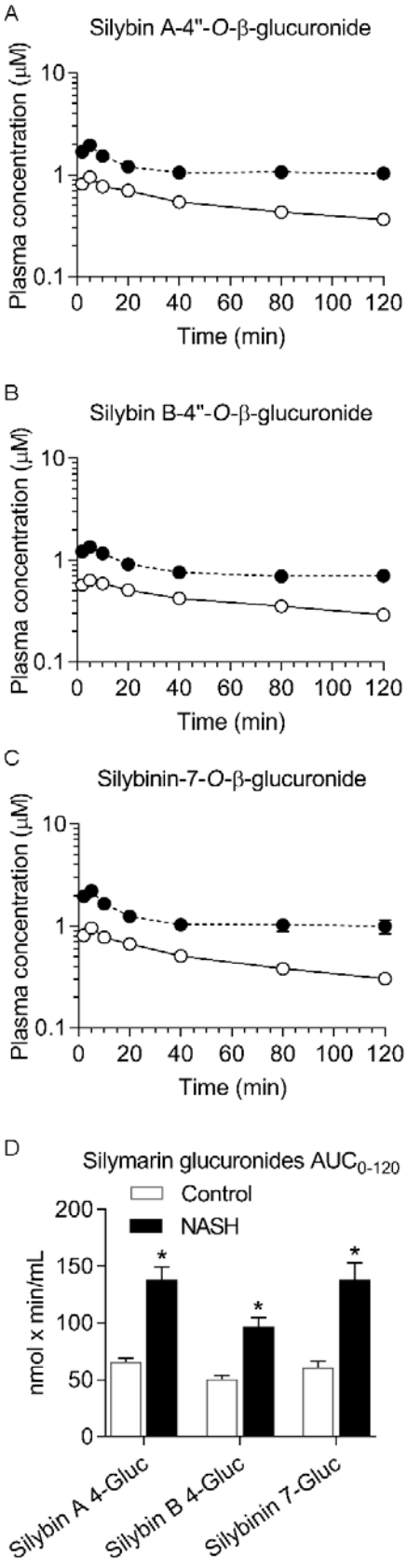

JPET Fast Forward. Published on August 16, 2019 as DOI: 10.1124/jpet.119.260489
This article has not been copyedited and formatted. The final version may differ from this version.

Figure 3

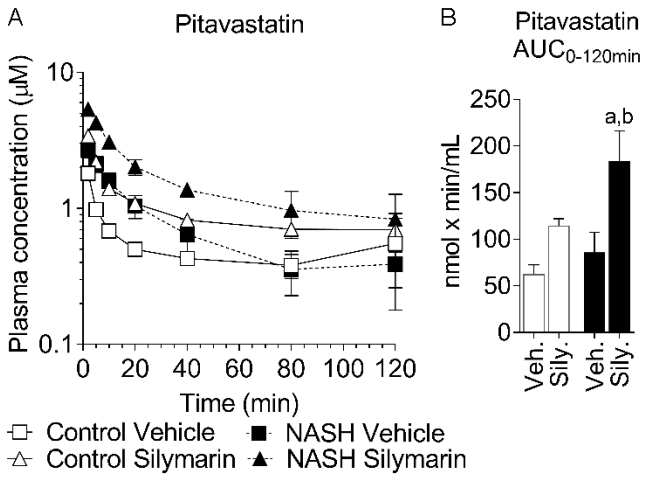

2-way ANOVA	Pitavastatin $AUC_{0\text{-}120min}$
NASH	**<0.05**
Silymarin	**<0.05**
Interaction	0.24

JPET Fast Forward. Published on August 16, 2019 as DOI: 10.1124/jpet.119.260489
This article has not been copyedited and formatted. The final version may differ from this version.

Figure 4

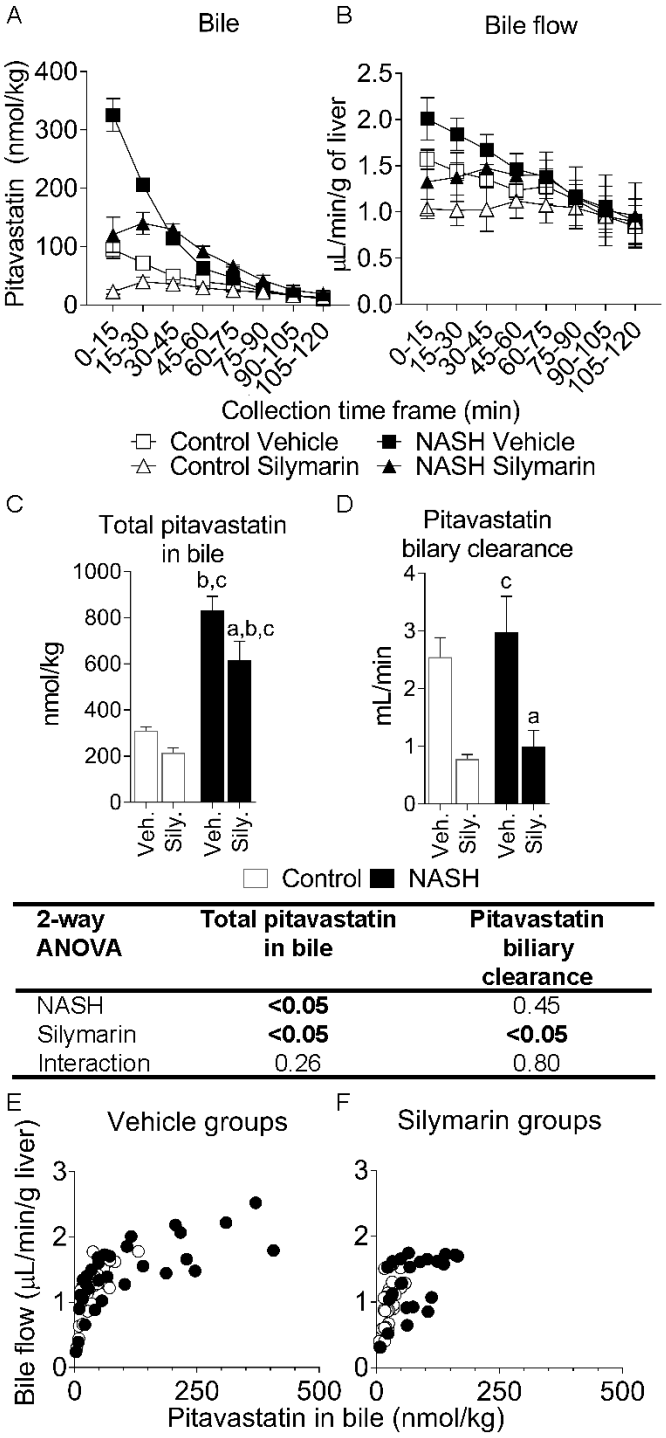

2-way ANOVA	Total pitavastatin in bile	Pitavastatin biliary clearance
NASH	**<0.05**	0.45
Silymarin	**<0.05**	**<0.05**
Interaction	0.26	0.80

JPET Fast Forward. Published on August 16, 2019 as DOI: 10.1124/jpet.119.260489
This article has not been copyedited and formatted. The final version may differ from this version.

Figure 5

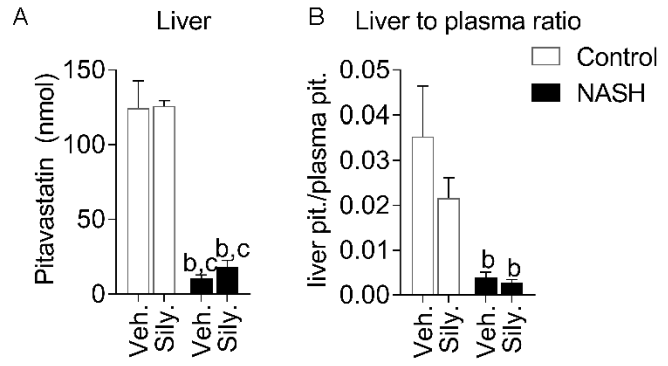

2-way ANOVA	Liver	Liver to plasma ratio
NASH	**<0.05**	**<0.05**
Silymarin	0.67	0.28
Interaction	0.79	0.36

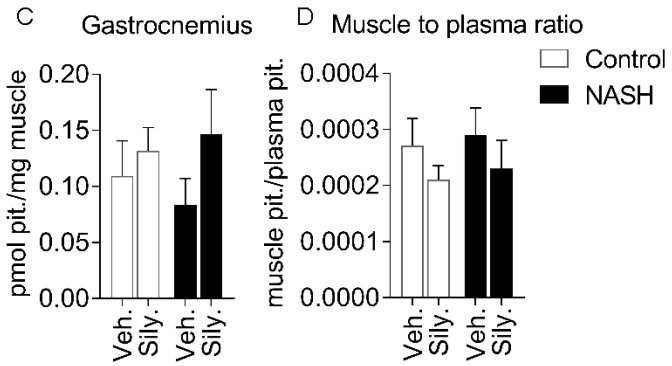

2-way ANOVA	Gastroc.	Muscle to plasma ratio
NASH	0.84	0.68
Silymarin	0.16	0.20
Interaction	0.49	0.99

JPET Fast Forward. Published on August 16, 2019 as DOI: 10.1124/jpet.119.260489
This article has not been copyedited and formatted. The final version may differ from this version.

Figure 6

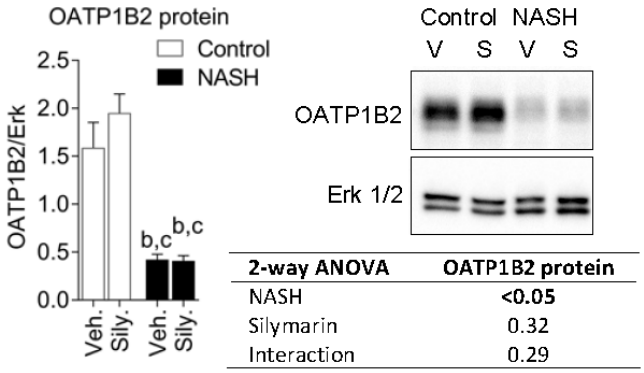

2-way ANOVA	OATP1B2 protein
NASH	**<0.05**
Silymarin	0.32
Interaction	0.29

JPET Fast Forward. Published on August 16, 2019 as DOI: 10.1124/jpet.119.260489
This article has not been copyedited and formatted. The final version may differ from this version.

Figure 7

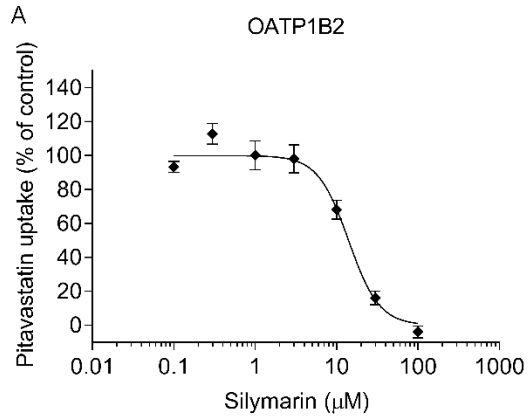

	OATP1B2	OATP1B1	OATP1B3
IC_{50} (μM)	13.8 ± 1.5	6.5 ± 2.2	12.7 ± 4.2

JPET Fast Forward. Published on August 16, 2019 as DOI: 10.1124/jpet.119.260489
This article has not been copyedited and formatted. The final version may differ from this version.

Figure 8